

Experimental observation of the effect of pulse duration on optical properties in ultrafast laser micro-processing of polymers



Cite as: J. Laser Appl. **33**, 042003 (2021); <https://doi.org/10.2351/7.0000462>

Submitted: 26 June 2021 . Accepted: 16 August 2021 . Published Online: 13 September 2021

Arifur Rahaman, Xinpeng Du, Aravinda Kar, Xiaoming Yu, et al.

COLLECTIONS

Note: Paper published as part of the special topic on Proceedings of the International Congress of Applications of Lasers & Electro-Optics 2021.

This paper was selected as Featured

This paper was selected as Scilight



[View Online](#)



[Export Citation](#)



[CrossMark](#)



ALIA THE LASER INSTITUTE **Journal of Laser Applications**

Special Issue: Laser Hybrid Manufacturing

READ NOW!

Experimental observation of the effect of pulse duration on optical properties in ultrafast laser micro-processing of polymers



Cite as: J. Laser Appl. **33**, 042003 (2021); doi: [10.2351/7.0000462](https://doi.org/10.2351/7.0000462)

Submitted: 26 June 2021 · Accepted: 16 August 2021 ·

Published Online: 13 September 2021



Arifur Rahaman,^{a)} Xinpeng Du, Aravinda Kar, and Xiaoming Yu

AFFILIATIONS

CREOL, The College of Optics and Photonics, University of Central Florida, Orlando, Florida 32816

Note: Paper published as part of the special topic on Proceedings of the International Congress of Applications of Lasers & Electro-Optics 2021.

^{a)}arahaman16@knights.ucf.edu

ABSTRACT

Polymers are important materials for both industrial and scientific applications. However, it is challenging to efficiently process polymers with an ultrafast laser due to their low melting point, high bandgap, and different absorption mechanics with different laser parameters. It is common practice in industries to use different kinds of lasers and, therefore, different laser parameters, such as pulse duration, wavelength, pulse energy, etc. In particular, the effect of pulse duration during ultrafast laser interaction with polymers is significant as the absorption mechanism can be different with different pulse durations. In this study, the effect of pulse duration is investigated during the ultrafast laser interaction with transparent polypropylene (TPP), which is an important polymeric material widely used in many industrial applications. This study is based on the experimental measurement of the optical properties of TPP during ultrafast interaction, where optical properties, i.e., reflectance, transmittance, and absorptance, are determined by performing time-resolved measurements in single-pulse configurations. This experiment is carried out by collecting *in situ* data of the reflection and transmission of each laser pulse in an ellipsoidal reflector-based experimental setup, which enables the collection of both specular and diffusive reflection with nearly full coverage, and absorption is calculated from the experimental results. It is found that TPP undergoes a dramatic morphological change with different pulse durations ranging from 167 fs to 1 ps, which is correlated with the change of optical properties during the ultrafast laser interaction with TPP for different pulse durations. This result will be useful for controlling the processing of polymers with ultrafast lasers for industrial applications.

Key words: polymer processing, ultrafast laser, effect of pulse during, pulse shaping, optical properties

Published under an exclusive license by Laser Institute of America. <https://doi.org/10.2351/7.0000462>

I. INTRODUCTION

In the last few years, ultrafast laser technologies have proved to be of great interest for material processing applications.¹⁻³ The interest in the ultrafast laser micro-processing of polymers has grown significantly over the past few years due to the high demand for using polymers in scientific and industrial applications.⁴⁻⁸ However, material processing with an ultrafast laser is quite complicated due to the dynamic behavior of the interaction between the ultrashort pulse and the polymeric material. Therefore, the ultrafast laser micro-processing of polymers with high precision and control is challenging for researchers.^{9,10}

A promising approach that can control laser-material interaction for high-precision material processing is the temporal pulse shaping of ultrashort pulses.¹¹ Researchers have already shown that temporal pulse shaping helps enhance optical properties, i.e., absorptance, of materials.^{12,13} These various studies have provided some understanding of the dynamics of laser-matter interactions, but most of the studies deal with the ultrafast laser ablation of dielectrics, especially pure silica, while ultrafast pulse shaping for polymer processing has been investigated less, even though polymers are one of the first materials to be processed by ultrafast lasers.^{14,15} However, the nature of absorption for near-infrared

laser beams has not been fully understood, and therefore, it remains challenging to process polymers with high energy efficiency.

In this study, the effect of pulse duration is investigated during the ultrafast laser interaction with a transparent PP sample in a single-shot configuration. An analytical solution of the differential equation of ultrafast laser pulse propagation is applied considering the spatial and temporal distributions of intensity to observe intensity distribution inside the sample. The enhancement of absorptance is investigated for different pulse durations by performing the time-resolved measurement of optical properties of the ultrafast laser-material interaction with polymer (i.e., polypropylene). Besides, the spatial and temporal distortions of ultrashort pulse propagation through the medium is investigated.

II. SPATIAL AND TEMPORAL DISTORTIONS OF ULTRASHORT PULSE

The equation, which describes the attenuation of the ultrafast laser pulse with spatial and radial intensity, $I(r, z, t)$, passing through the material undergoing single-photon, two-photon, or two-step absorption or three-photon or three-step absorption, is given by

$$\frac{dI(r_i, z_i, t)}{dz_i} = -\alpha_1 I(r_i, z_i, t) - \alpha_2 I^2(r_i, z_i, t) - \alpha_3 I^3(r_i, z_i, t), \quad (1)$$

where α_1 , α_2 , and α_3 are the linear, two-photon, or two-step nonlinear absorption coefficient and three-photon or three-step nonlinear absorption coefficient, respectively. Here, $i = 1, 2, 3$, etc. are considered for multiple reflection cases.

The analytical solution of the above differential equation, after passing through the material, can be expressed below, which is given in greater detail elsewhere:¹⁶

$$I_{ii}(r_i, z_i, t) = \frac{1}{3a_i(r_i, z_i, t)} \left(Q_i(r_i, z_i, t) + \frac{\Delta_{oi}(r_i, z_i, t)}{Q_i(r_i, z_i, t)} - b_i(r_i, z_i, t) \right), \quad (2)$$

where $I_{ii}(r_i, L_i, t)$ is the incident intensity at the different interfaces except for the first incident point. All the variables in the above equation are defined elsewhere.¹⁶

The study of the propagation of an optical Gaussian pulse is important to control the process with an ultrafast laser. When a high-intensity ultrafast laser pulse propagates through an optical medium, the Gaussian pulse intensity is distorted temporally and spatially during the propagation due to the nonlinear phenomena, i.e., the nonlinear refractive index changes due to an intense pulse. To investigate the distortion of the Gaussian pulse, Eq. (2) is used, and the intensity distribution is shown in Fig. 1.

Figure 1(a) shows the spatial distribution of the peak intensity of the ultrashort pulse during propagation through the transparent PP sample. It can be seen that the peak intensity of the Gaussian pulse reduces by 70% within 50 μm distance inside the transparent sample and the shape of the Gaussian pulse changes to a different pulse shape, which is close to the flat top close to the back (exit) surface of the sample, where the sample thickness is around

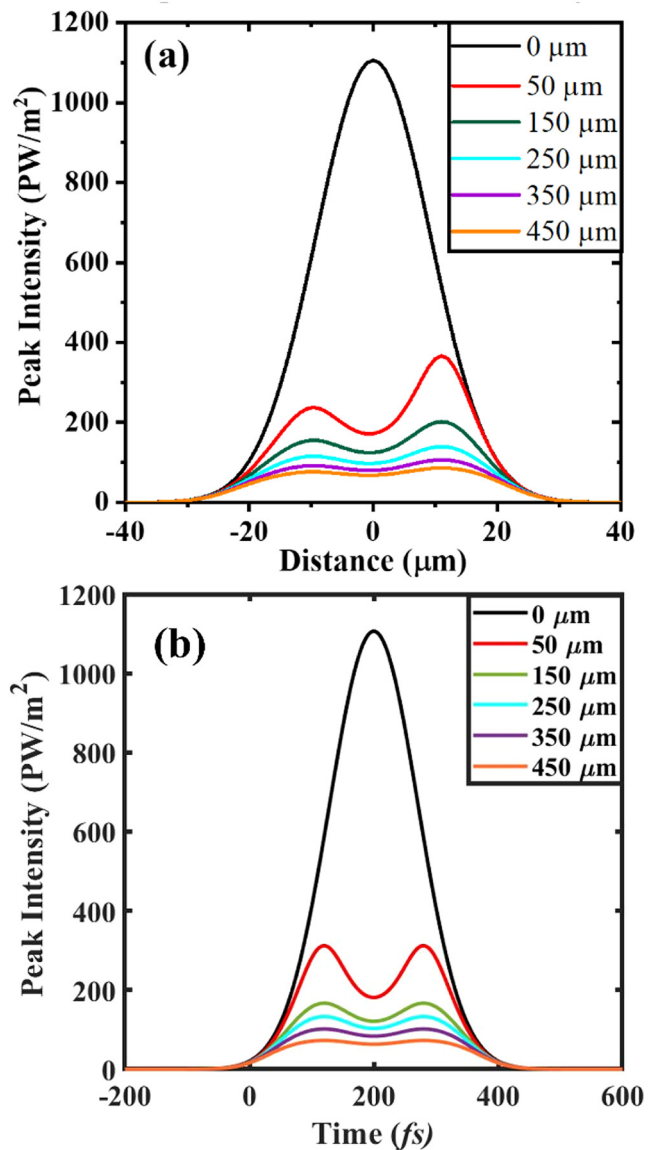


FIG. 1. (a) Spatial distribution and (b) temporal distribution of the peak intensity of the ultrafast laser with a pulse duration of 167 fs.

450 μm . Similarly, the temporal distortion of the peak intensity is shown in Fig. 1(b).

The distribution of the peak intensity has two peaks at different axial distances of the sample, and the difference in the height of the peaks decreases as the pulse propagates through the medium because the high-intensity pulse gets more distorted than the low-intensity one as it propagates through the medium. It can be seen that the peaks are not the same in the spatial distribution case, where the possible reason for this spatial distribution is the incident angle of the laser beam at the sample and two peaks of the spatial

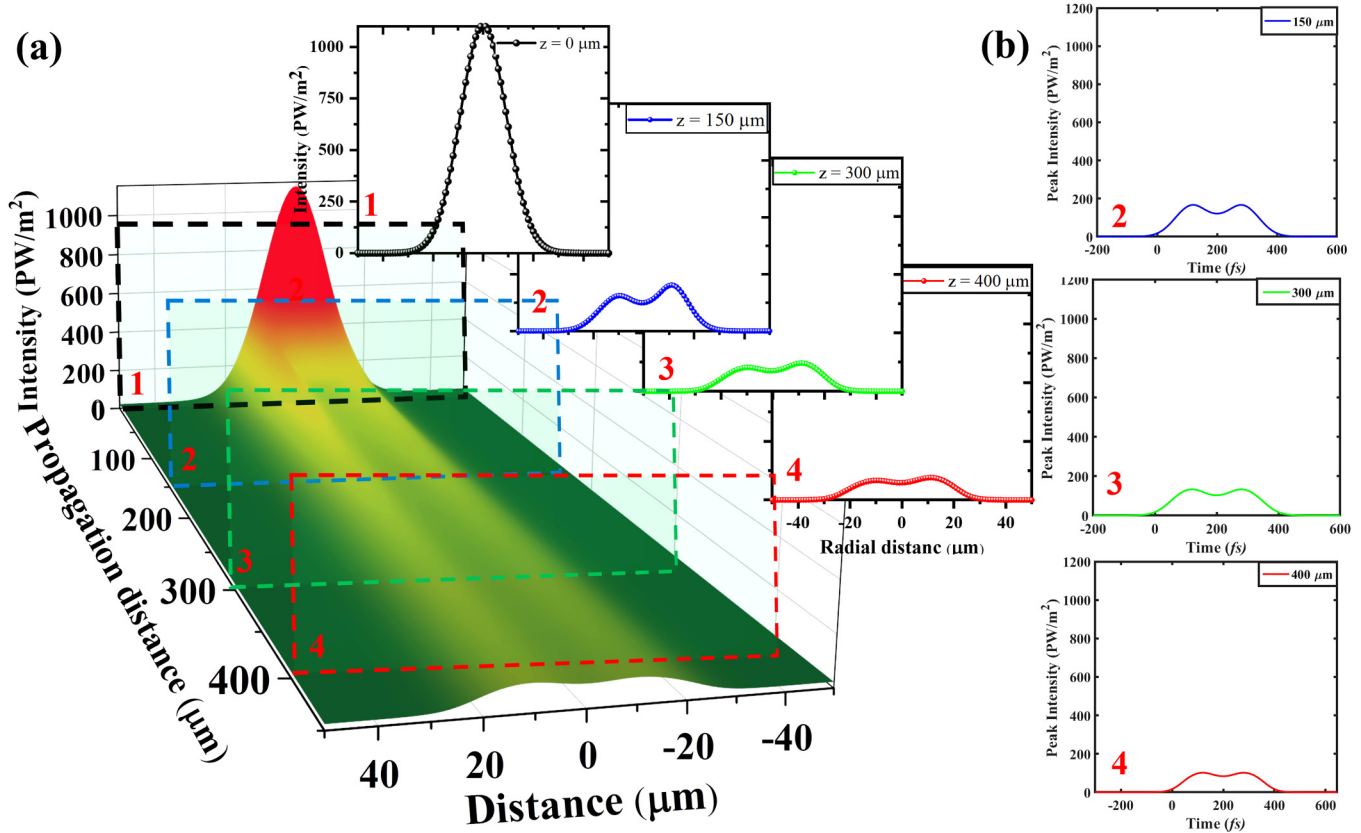


FIG. 2. (a) 3D representation of the spatial distribution of peak intensity of ultrafast laser during propagation through the transparent PP sample and (b) the temporal distribution of the peak intensity corresponding to 2, 3, and 4 of (a).

distribution of the peak intensity appear due to the nonlinear refractive index change during high-intensity propagation. Figure 2 shows the distribution of the peak intensity at a different axial distance inside the medium with a pulse duration of 167 fs, where the distribution of the peaks also displays similar behavior to the spatial case.

III. EFFECT OF PULSE DURATIONS

To investigate the effect of the pulse duration on ultrafast laser interaction with the PP sample, different experiments are performed with a single pulse configuration for a wide range of pulse energies (1–100 µJ) and different pulse durations, i.e., 167, 371, 710, and 1000 fs.

Figure 3 shows the front surface damage with different pulse energies (1–100 µJ) and pulse durations (i.e., 167, 371, 710, and 1000 fs). The front surface damage is dominant for 167 fs since most of the energy is absorbed at the surface of the sample due to high peak intensity, which has a higher nonlinear effect. Figure 4 shows the back surface damage with different pulse energies and pulse durations. Here, the back surface (or the exit

surface) damage is dominant in the case of a longer pulse duration (i.e., 1000 fs for this study), and there is back surface damage for the 167 fs pulse duration as mentioned above because most of the energy is absorbed at the front surface for a shorter pulse case (i.e., 167 fs).

Figure 5(a) shows the determination of the damage area created by a single pulsed laser shot from the optical microscopic image of damage, and Fig. 5(b) shows the semilog graph of the damage area as a function of peak intensities. This graph is used to determine the peak damage threshold intensity corresponding to the different pulse durations, where the highest peak threshold damage intensity is found to be 12.9 TW/cm² with a shorter pulse duration (i.e., 167 fs), and the lowest peak threshold damage intensity is obtained as 4.1 TW/cm² with longer pulse durations (i.e., 1000 fs). However, in the case of peak damage threshold fluence, the highest value is obtained as 5.1 J/cm² for the longest pulse duration, which is shown in Fig. 6, and the lowest damage threshold fluence is found to be 1.2 J cm⁻² for 167 fs.

The relation between the peak damage threshold fluence and the pulse duration can be explained with simple scaling laws derived by Gamaly *et al.*¹⁷ as $F_{th} \sim t_{on}^\eta$, where η can be found from

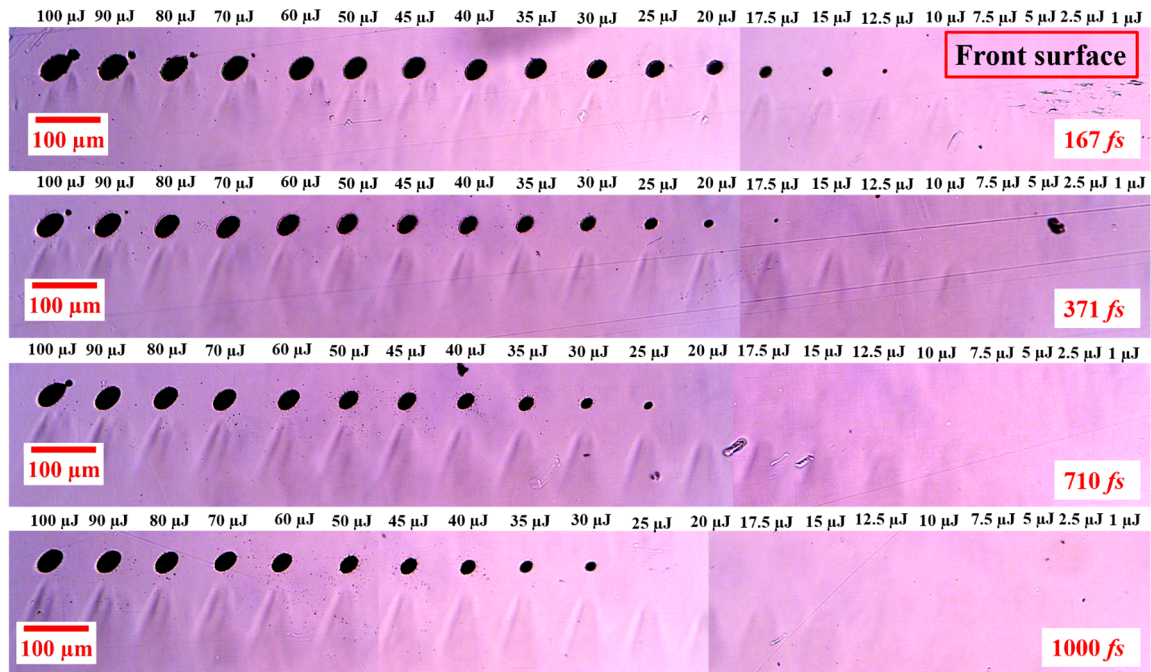


FIG. 3. The front surface damage of the transparent PP sample with different pulse durations (i.e., 167, 371, 710, and 1000 fs) for a wide range of pulse energies (1–100 μJ).

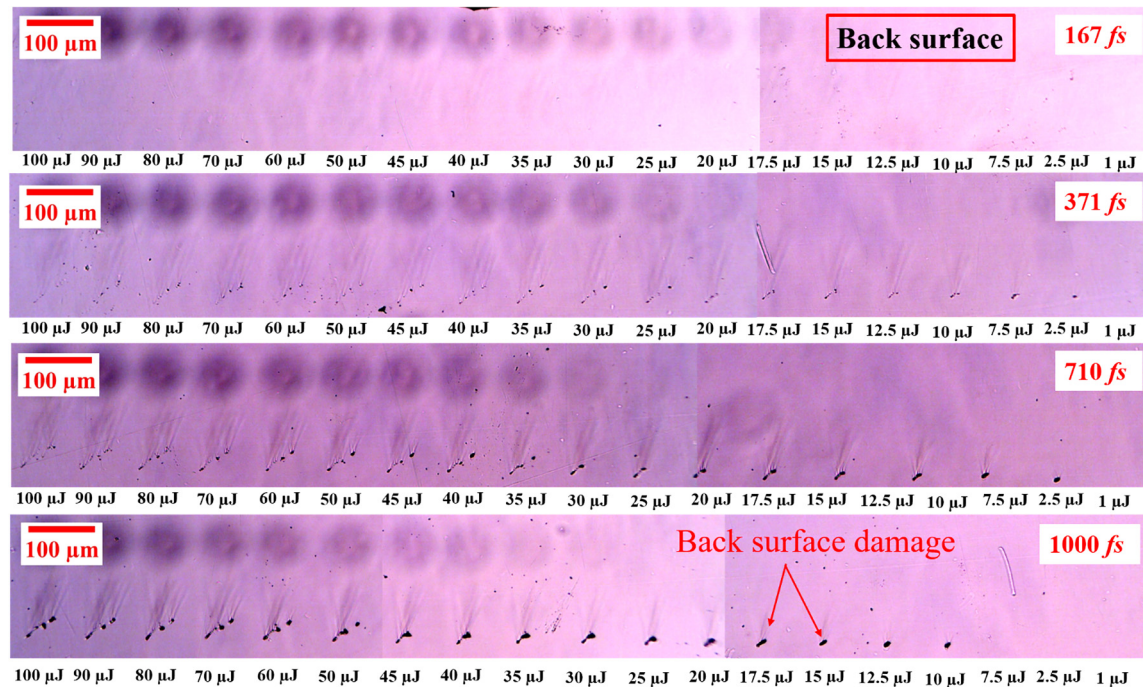


FIG. 4. The back surface damage of the transparent PP sample with different pulse durations (i.e., 167, 371, 710, and 1000 fs) for a wide range of pulse energies (1–100 μJ).

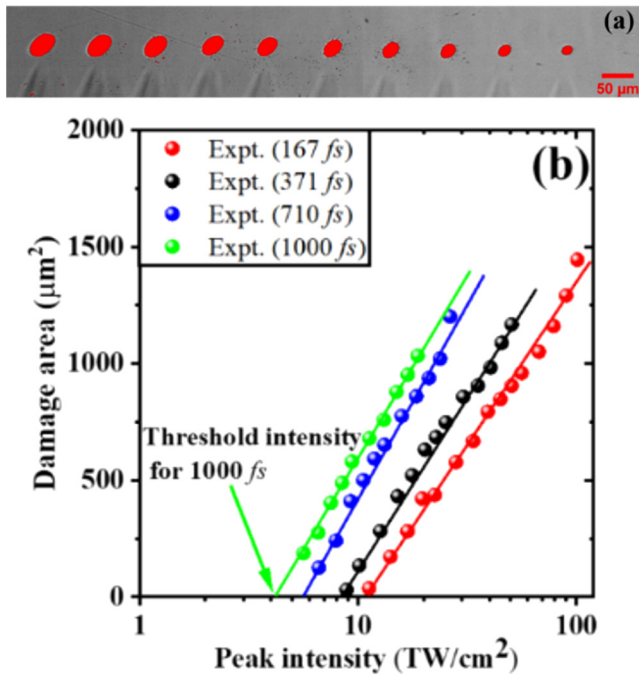


FIG. 5. Determining (a) the damage area from optical microscopic images for different pulse durations (i.e., 167, 371, 710, and 1000 fs) and (b) the damage threshold peak intensity with different pulse durations (i.e., 167, 371, 710, and 1000 fs).

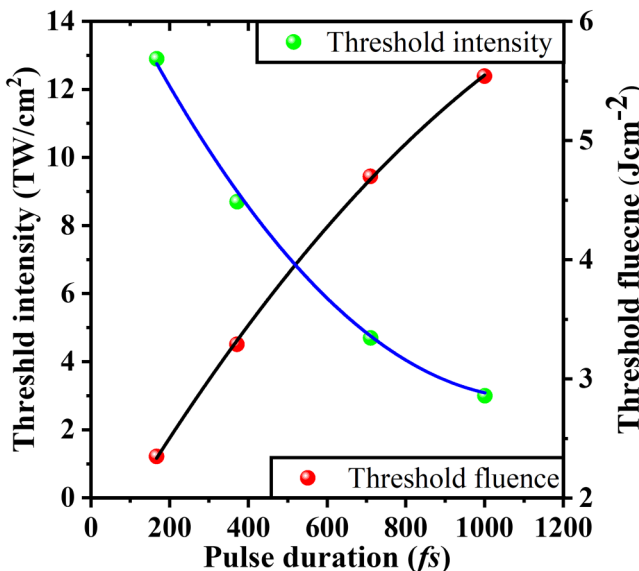


FIG. 6. The damage threshold peak fluence/intensity with different pulse durations.

the fitting of damaged peak fluence as a function of pulse duration (t_{on}), which is found to be $\eta = 0.23$ in this study, which is similar to the literature value for shorter pulse cases.¹⁸ Similarly, the relation between the peak damaged threshold intensity and the pulse duration can be expressed as $I_{th} \sim F_{th}/t_{on}$.

To compare the front surface damage area that is determined from the experimental results, the damage areas from different pulse durations are theoretically determined by using the following equation:

$$A = \frac{1}{2} \pi \omega_0^2 \ln \left(\frac{I_o}{I_{th}} \right), \quad (3)$$

where $I_o = 2E_p/\pi\omega_0^2 t_{on}$ and I_{th} are the incident peak intensity and the peak damaged threshold intensity, respectively. The peak damaged threshold intensity is obtained from Fig. 7. Figure 7 shows the damaged area as a function of peak intensity and peak fluence for different pulse durations. Smaller types of damage are obtained with lower fluences, which agree with those in the literature.¹⁹ The theoretical calculation shows a good match with experimental results, except for high intensities and shorter pulse durations, where the peak intensity is too high, which leads to the creation of air ionization or other nonlinear phenomena that are not considered in this calculation.

IV. EFFECT OF PULSE DURATION ON ULTRAFAST LASER INTERACTION

Figure 8 shows the front and back surface damage with a 1000fs pulse duration. For the 1000 fs pulse duration case, a strong back surface damage is observed with a pulse energy $<30 \mu\text{J}$, although the front surface damage appears at $30 \mu\text{J}$ and no front surface damage is observed at $<30 \mu\text{J}$. A possible reason could be the electric-field enhancement at the exit side and self-focusing due to the nonlinear refractive index change with an ultrafast laser pulse.

When light travels from a lower refractive index medium to a higher refractive index medium, the reflected electric field undergoes a phase shift of 180° in relation to the incident light wave. For traveling from a higher refractive index to a lower index medium, the reflected electric field undergoes a zero (0°) phase shift. To verify the electric field enhancement at the exit surface, Crisp *et al.*²⁰ gave a simple expression as follows:

$$\frac{S_{\text{ent}}^D}{S_{\text{exit}}^D} = \frac{4n^2}{(n+1)^2}, \quad (4)$$

where S_{ent}^D is the incident power per unit area that corresponds to damage of the entrance face and S_{exit}^D is the incident power per unit area that corresponds to the damage of the entrance face. Since the Rayleigh length in this study is larger than the thickness of the sample ($450 \mu\text{m}$), and with the assumption of no self-focusing and the same beam diameter at the exit surface as the front surface, Eq. (4) can be written as follows:

$$\frac{E_{\text{ent}}^D}{E_{\text{exit}}^D} = \frac{4n^2}{(n+1)^2}, \quad (5)$$

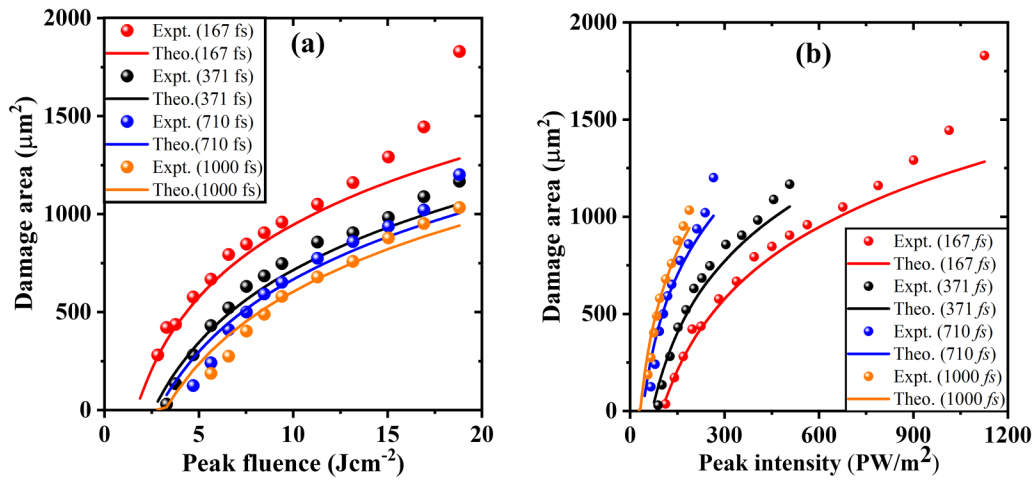


FIG. 7. Comparing the theoretical and experimental damaged areas as a function of (a) peak fluence and (b) peak intensity.

where E_{ent}^D and E_{exit}^D are the threshold pulse energies at the entrance surface and threshold pulse energy at the exit surface, respectively, which are shown in Fig. 9. Here, the left side of Eq. (5) is found to be $E_{ent}^D/E_{exit}^D = 4$ from the experimental results and the right-hand side is found to be 1.44 (where the linear refractive index is 1.44). Therefore, Eq. (4) is not satisfied properly with our experimental results. To obtain information on the diameter of the laser beam at the front and back surfaces from our experimental results, the damaged area at the front and back is plotted with $M = \ln(2E_p/t_{on}I_{th})$ and Eq. (6) is used to fit the experimental data,

$$\pi\omega_{damage}^2 = \pi\omega_{beam}^2 \ln\left(\frac{2E_p}{t_{on}I_{th}}\right) - \pi\omega_{beam}^2 \ln(A). \quad (6)$$

The ratio of the entrance beam radius and the back surface beam radius is found to be 3.72 ($r_{entrance}/r_{exit} \approx 3.72$) from the slope value, $\pi\omega_{beam}^2$, of the above in Figs. 7 and 10. This result indicates that the diameter of the beam at the back surface is smaller than the beam diameter at the front surface. To verify this result, a simple experiment is designed to measure the beam diameter at the front surface (without any sample) and the beam diameter at the back surface of the sample for single-pulse configuration by triggering the pulse. Figure 11 shows the camera images at the front surface (without sample) and the back (exit) surface of the sample, which also indicate that the beam diameter at the back surface is much smaller than that at the front surface. From these experimental verifications, it is obvious that the field enhancement might not be the only reason for the back surface damage, and there might be

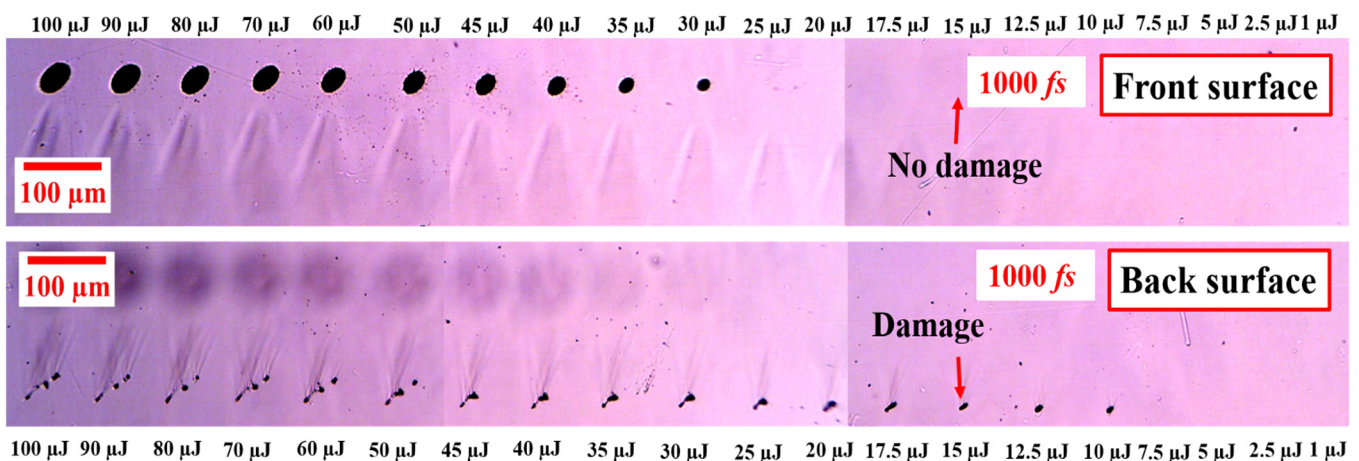


FIG. 8. Front and back surface damage with a 1000 fs pulse duration.

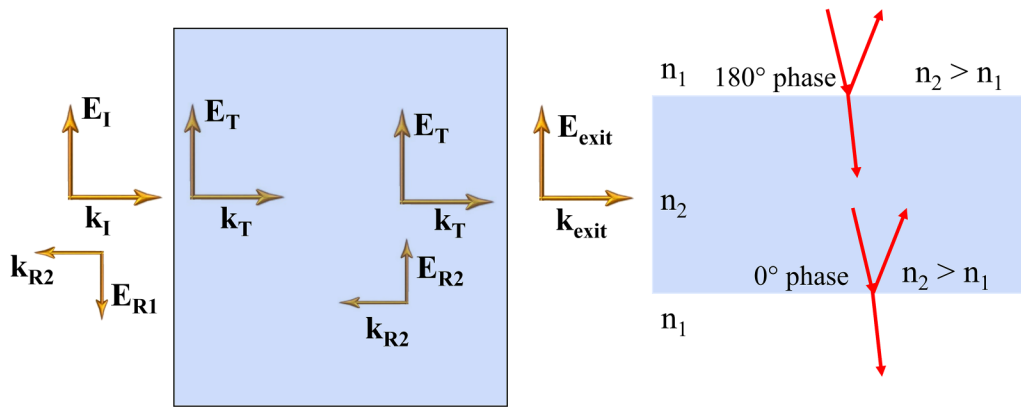


FIG. 9. Electric fields at the entrance and back surfaces of a polymer surface. An incident angle is considered at a normal incident.

a self-focusing effect^{21,22} that leads to a strong back surface damage during longer pulse durations as the energy is not absorbed at the front surface of the sample during laser-matter interaction.

V. EFFECT ON OPTICAL PROPERTIES

Figure 12 shows the reflectance (R), transmittance (T), and absorbance (A) as a function of the peak fluences for different pulse durations (i.e., 167, 371, 710, and 1000 fs). As mentioned above, the single-shot experiment is performed to see the effect of the pulse duration for a wide range of pulse energies from 1 to 100 μJ , which correspond to the fluence of 0.94–18.8 J cm^{-2} . Figure 12(a) shows the reflectance of the transparent PP sample as a function of the peak fluence of the incident laser beam, where reflectances are very low as the sample is mostly transparent. Note that the tolerance of this measurement is about ± 0.012 . Figure 12(a) shows that the reflectance with different pulse durations is within the tolerance limit, which indicates that the reflectance is not much dependent on pulse duration for a transparent PP sample case. It can be seen that the reflectance starts to decrease after a certain value of fluence from which the nonlinear absorption mechanism starts.

Figures 12(b) and 12(c) show the transmittance (T) and absorbance of the ultrafast laser beam through the transparent PP sample. At low fluences, the transmittances for all pulse durations have almost constant values, which indicates the linear absorption mechanism with low fluences. The transmittance starts to decrease after certain fluences, where nonlinear absorptions start to happen. However, the transmittance starts decreasing first for the 167 fs pulse duration due to the high peak intensity leading to a nonlinear absorption with a lower fluence that also supports the damage morphology shown in Figs. 3 and 4. Although the peak intensity for the case 1000 fs is less, transmittance starts to decrease earlier than the 371 and the 710 fs cases, which might be the reason for the strong back surface damage shown in Fig. 8.

Figure 12(c) shows the absorbance during the ultrafast laser interaction with a transparent PP sample, which is determined

from the experimental value of transmittance and reflectance as $A = 1 - T - R$. As the reflectance of this study is very small, the transmittance has a dominant effect in determining absorbance. As explained in the transmittance case, for a low fluence, the absorbance is constant for linear absorption mechanisms and starts to increase after a certain level of fluence (i.e., 1 J cm^{-2} for the 167 fs pulse duration).

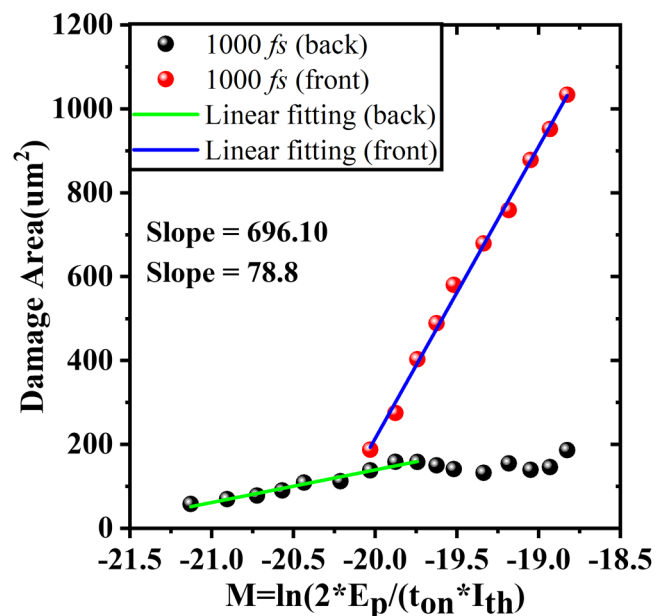


FIG. 10. Determining the beam diameter at the front and the back surfaces from an experimental damage diameter.

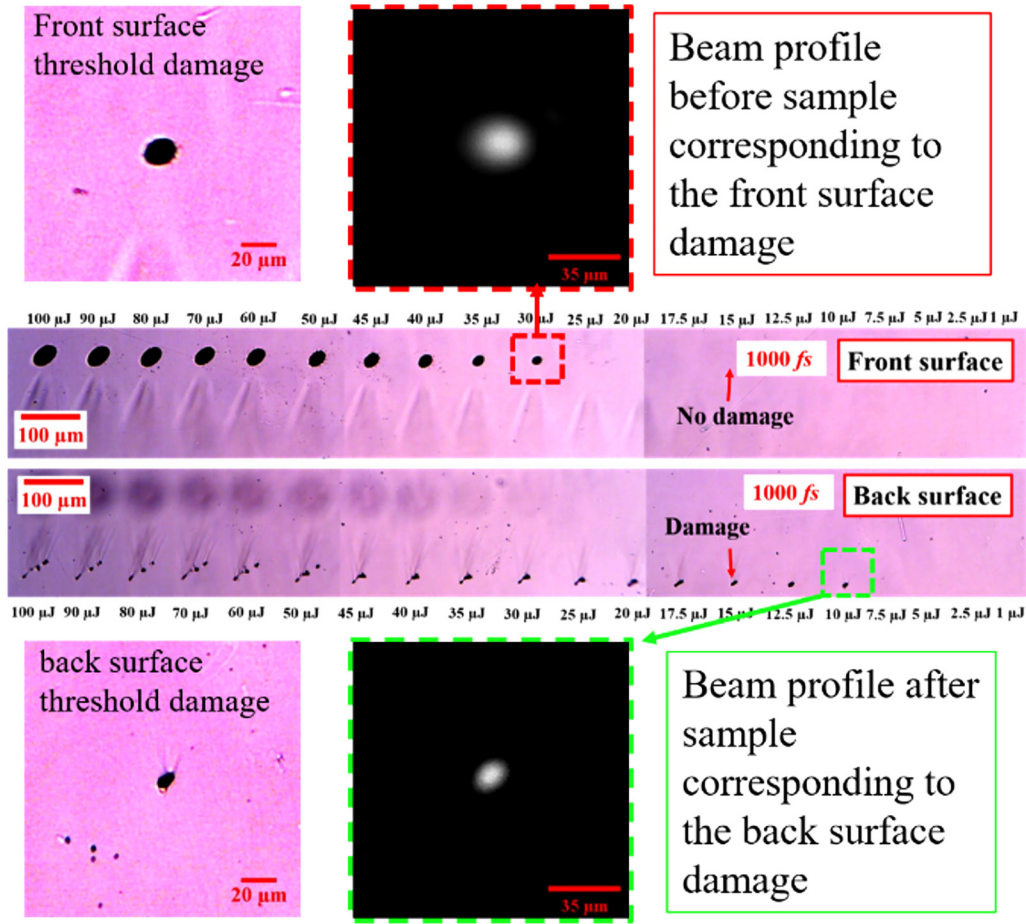


FIG. 11. Camera image of the beam diameter at the entrance surface and the exit surface.

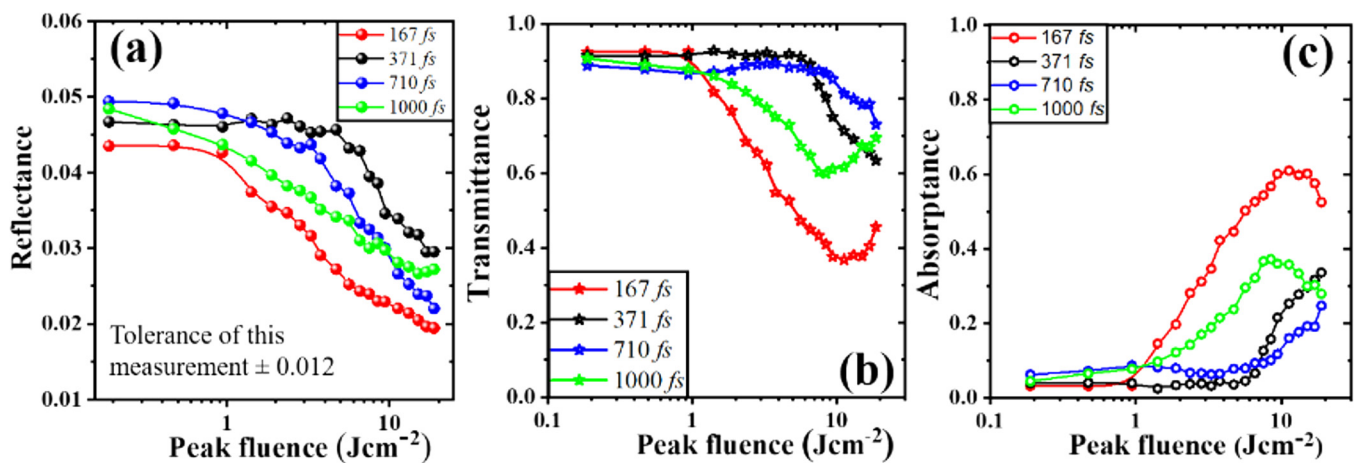


FIG. 12. (a) Reflectance (R), (b) transmittance (T), and (c) absorbance (A) as a function of laser fluences with different pulse durations (i.e., 167, 371, 710, and 1000 fs).

VI. CONCLUSIONS

The effect of the pulse duration is investigated both experimentally and theoretically. This study showed the most effective energy region for processing transparent PP samples with ultrafast lasers with different pulse durations. The shorter pulse duration (167 fs) is preferred for surface processing, while longer pulses (~1 ps) create subsurface and back surface damage. The back surface damage with 1000 fs is suggested to happen due to self-focusing phenomena, which have a lower critical power for a longer pulse. This study also shows that the shorter pulses have higher distortion than the longer pulse inside the material and that most absorptances that happen for the shorter pulse is at the surface of the material.

ACKNOWLEDGMENTS

Financial support from Elsner Engineering Works is appreciated.

REFERENCES

- ¹K. Sugioka and Y. Cheng, "Ultrafast lasers—reliable tools for advanced materials processing," *Light: Sci. Appl.* **3**, 1–12 (2014) e149.
- ²R. R. Gattass and E. Mazur, "Femtosecond laser micromachining in transparent materials," *Nat. Photonics* **2**, 219–225 (2008).
- ³K. C. Phillips, H. H. Gandhi, E. Mazur, and S. K. Sundaram, "Ultrafast laser processing of materials: A review," *Adv. Opt. Photonics* **7**, 684–712 (2015).
- ⁴A. Shibata, S. Yada, and M. Terakawa, "Biodegradability of poly (lactic-co-glycolic acid) after femtosecond laser," *Sci. Rep.* **6**, 1–9 (2016).
- ⁵M. Terakawa, "Femtosecond laser processing of biodegradable polymers," *Appl. Sci.* **8**, 1123 (2018).
- ⁶A. Rahaman, A. Kar, and X. Yu, "Thermal effects of ultrafast laser interaction with polypropylene," *Opt. Express* **27**, 5764–5783 (2019).
- ⁷A. Rahaman, X. Du, B. Zhou, H. Cheng, A. Kar, and X. Yu, "Absorption and temperature distribution during ultrafast laser micro-cutting of polymeric materials," *J. Laser Appl.* **32**, 022044 (2020).
- ⁸B. Zhou, A. Rahaman, X. Du, H. Cheng, A. Kar, and X. Yu, "Laser processing of dielectrics using spatiotemporally tuned ultrashort pulses," *J. Laser Appl.* **32**, 022041 (2020).
- ⁹K. Sugioka, "Progress in ultrafast laser processing and future prospects," *Nanophotonics* **6**, 393–413 (2017).
- ¹⁰M. V. Shugaev, C. Wu, O. Armbruster, A. Naghilou, N. Brouwer, D. S. Ivanov, T. J. Y. Derrien, N. M. Bulgakova, W. Kautek, B. Rethfeld, and L. V. Zhigilei, "Fundamentals of ultrafast laser-interaction," *MRS Bull.* **41**, 960–968 (2016).
- ¹¹F. Bourquard, J. P. Colombier, M. Guillermin, A. S. Loir, C. Donnet, R. Stoian, and F. Garrelie, "Temporal pulse shaping effects on aluminum and boron ablation plumes generated by ultrashort pulsed laser ablation and analyzed by time- and space-resolved optical spectroscopy," *Appl. Surf. Sci.* **258**, 9374–9378 (2012).
- ¹²R. Stoian, M. Boyle, A. Thoss, A. Rosenfeld, G. Korn, I. V. Hertel, and E. E. B. Campbell, "Laser ablation of dielectrics with temporally shaped femtosecond pulses," *Appl. Phys. Lett.* **80**, 353–355 (2002).
- ¹³M. Spyridaki, E. Koudoumas, P. Tzanetakis, and C. Fotakis, "Temporal pulse manipulation and ion generation in ultrafast laser ablation of silicon," *Appl. Phys. Lett.* **84**, 1474–1476 (2003).
- ¹⁴S. Kuper and M. Stuke, "Femtosecond UV excimer laser ablation," *Appl. Phys. B* **44**, 199–204 (1987).
- ¹⁵R. Srinivasan, E. Sutcliffe, and B. Braren, "Ablation and etching of polymethylmethacrylate by very short (160 fs) ultraviolet (308 nm) laser pulses," *Appl. Phys. Lett.* **51**, 1285–1287 (1987).
- ¹⁶A. Rahaman, X. Du, B. Zhou, A. Kar, and X. Yu, "Pulse-to-pulse evolution of optical properties in ultrafast laser micro-processing of polymers," *J. Laser Appl.* **33**, 012020 (2021).
- ¹⁷E. G. Gamaly, A. V. Rode, B. Luther-Davies, and V. T. Tikhonchuk, "Ablation of solids by femtosecond lasers: Ablation mechanism and ablation threshold for metals and dielectrics," *Phys. Plasmas* **9**, 949–957 (2002).
- ¹⁸M. D. Crisp, N. L. Boling, and G. Gube, "Importance of Fresnel reflections in laser surface damage of transparent dielectrics," *Appl. Phys. Lett.* **21**, 364–366 (1972).
- ¹⁹A. Bendib, K. Bendib-Kalache, and C. Deutsch, "Optical breakdown threshold in fused silica with femtosecond laser pulses," *Laser Part. Beams* **31**, 523–529 (2013).
- ²⁰B. N. Chichkov, C. Momma, S. Nolte, F. V. Alvensleben, and A. Tunnermann, "Femtosecond, picosecond and nanosecond laser ablation of solids," *Appl. Phys.* **63**, 109–115 (1996).
- ²¹S. Butkus, E. Gaizauskas, L. Macernyte, V. Jukna, D. Paipulas, and V. Sirutkaitis, "Femtosecond beam transformation effects in water, enabling increased throughput micromachining in transparent materials," *Appl. Sci.* **9**, 2405 (2019).
- ²²D. M. Rayner, A. Naumov, and P. B. Corkum, "Ultrashort pulse non-linear optical absorption in transparent media," *Opt. Express* **9**, 3208–3217 (2005).